Received: 22 March 2019 | Revised: 10 June 2019 | Accepted: 18 June 2019

DOI: 10.1002/ces2.10015

ORIGINAL ARTICLE

International Journal of Ceramic Engineering & Science

Effects of processing parameters on 3D structural ordering and optical properties of inverse opal photonic crystals produced by atomic layer deposition

Heloisa G. Campos[1] | **Kaline P. Furlan**[2,3] | **Daniel E. Garcia**[1] | **Robert Blick**[3] | **Robert Zierold**[3] | **Manfred Eich**[4,5] | **Dachamir Hotza**[1] | **Rolf Janssen**[2]

[1]Graduate Program in Materials Science and Engineering (PGMAT), Federal University of Santa Catarina (UFSC), Florianópolis, Brazil

[2]Institute of Advanced Ceramics, Hamburg University of Technology (TUHH), Hamburg, Germany

[3]Institute of Nanostructure and Solid-State Physics and Center for Hybrid Nanostructures, Universität Hamburg, Hamburg, Germany

[4]Institute for Optical and Electronic Materials, Hamburg University of Technology, Hamburg, Germany

[5]Institute of Materials Research, Helmholtz-Zentrum Geesthacht, Geesthacht, Germany

Correspondence
Rolf Janssen, Institute of Advanced Ceramics, Hamburg University of Technology, Hamburg 21073, Germany.
Email: janssen@tuhh.de

Funding information
SFB 986 Hamburg University of Technology, Grant/Award Number: DXX/3264/SFB/1986/M09/C5

Abstract

Vertical convective self-assembly has been extensively used for the preparation of direct photonic crystals, which can be later infiltrated with a more stable material, such as oxide ceramics, by atomic layer deposition. However, the relationship between the self-assembly parameters of the direct photonic crystals and the optical properties of the inverse opal photonic crystals remains elusive. In this work, the effect of different experimental parameters on the 3D structure and the density of defects of polystyrene direct photonic crystals produced by vertical convective self-assembly was assessed. Self-assembly was investigated using deionized water as media with polymer particles' concentrations up to 2 mg/mL; temperatures of 40, 50, and 80°C; and relative humidity of 45%, 70%, and 90%. The 3D structure of the resultant direct photonic materials was characterized by the combination of scanning electron microscopy and image analysis, and their optical properties were assessed by reflectance measurements. These results were correlated with the performance of oxide-based inverse opal photonic crystals produced by the controlled infiltration of the former direct photonic crystals by atomic layer deposition (ALD). It was found that the thickness increased with the concentration of polystyrene particles, while the photonic structure ordering is dependent on the synergy between humidity and temperature. Results also showed higher defects population with increasing evaporation temperature and decreasing relative humidity.

KEYWORDS

3D structure, optical properties, photonic materials, vertical convective self-assembly

1 | INTRODUCTION

Self-assembly is a process whereby individual components arrange themselves into an ordered structure. In a self-assembled structure, the building blocks are usually linked by weak forces such as van der Walls, electrostatic, hydrogen bonds, hydrophobic, and stacking interactions as well as steric forces.[1] Application of self-assembly techniques requires highly ordered photonic crystals, such as optical fibers, lasers, photovoltaic cells, and other optoelectronic devices.[2–6]

Colloidal crystals can be self-assembled from a colloidal suspension by evaporation of the liquid solvent or by gravity sedimentation in a variety of approaches,[7] such as spin coating,[8] vertical deposition,[9,10] electrophoresis,[11,12] centrifugation,[13] freezing,[14] physical confinement,[15] or convective self-assembly[16] to name a few of them.

Vertical deposition is the method most extensively applied to produce outsized scale colloidal crystals. Novel functional nanomaterials such as photonic materials with tailor-made thickness have been obtained using a bottom-up fabrication approach.[17–19] However, depending on the type and the extent of the defects, colloidal crystals may suffer from reduced reflectance capability or no photonic band gap making them unusable for applications.[20] Typical defects may include line defects, point defects, drying cracks, stacking faults, and random variations in the sphere positions.[21,22] Thus, the creation of defect-free three-dimensional (3D) photonic crystals remains still challenging, although several reports for the production of photonic crystals by colloidal self-assembly have been published. During the self-assembly process, the colloidal crystal growth is affected by particle concentration, liquid evaporation rate, and the interparticle forces in the suspension.[5] As analyzed by Kuai et al,[22] evaporation temperature and relative humidity—both parameters influence the crystal growth rate by changing the evaporation rate of the solvent—have a strong influence on the film thickness, defects, and cracks. Those parameters were also analyzed by Liu et al,[5] who observed that lowering the evaporation temperature and increasing the relative humidity during the assembly process lead to the formation of high-quality crystals.

The effect of the suspension concentration on defective area is well reported in the literature. Yan et al,[15] Xiao et al,[1] and Weiss et al[23] showed that the density of defects increases for higher polymer concentration. Moreover, Zhang et al[21] and Voitchovsky et al[24] reached similar results when studying the correlation between the type of liquid used and the amount of defects. Additionally, Voitchovsky et al[24] revealed that the density of defects can be decreased by using higher polar solvents to lower the evaporation rate. In this paper, direct photonic crystals were produced on sapphire substrates via vertical convective self-assembly of polystyrene particles from aqueous suspensions. A systematic study of self-assembly parameters, namely suspension concentration, processing temperature, and relative humidity, was performed. The influence of these factors on the defect density and photonic structure ordering was assessed by scanning electron microscopy and spectroscopy techniques, respectively. These results were correlated with the performance of oxide-based inverse opal photonic crystals produced by controlled infiltration of the former direct photonic crystals by atomic layer deposition.

2 | MATERIALS AND METHODS

Monodisperse polystyrene (PS) particles (microparticles), with diameter of (0.76 ± 0.02) μm, were self-assembled on single crystal sapphire substrates (25 × 30 × 0.53 mm, Crystec). Vertical convective self-assembly (VCSA) was performed inside a humidity chamber (HCP 108, Memmert) for 120 hours, or until the complete evaporation of the solvent using Teflon beakers containing PS suspensions in filtered deionized water. The angle between the substrate normal and the beaker base was kept at 81° to 84°.

Colloidal crystal films were obtained by controlled evaporation of the liquid and different combinations of PS concentration (1, 1.5, 2 mg/mL), temperature (40, 55, 80°C), and relative humidity (RH) (45%, 70%, 90%).

After vertical colloidal self-assembly, thickness and structural morphology of the resulting direct photonic crystals were investigated by scanning electron microscopy (SEM, Leo 1530). The self-assembly defects were evaluated by image analysis (ImageJ, 1.51p22) in a minimum of 20 SEM images taken at lower magnification (500×). For elimination of noise (coming from the shadowing in between the spheres), a Gaussian filter was applied, with no loss of information concerning the defects. After binarization, the area of the defect was analyzed by an automated threshold definition.

Atomic layer deposition (ALD) of Al_2O_3 using the precursors trimethylaluminum (TMA, Sigma-Aldrich) and deionized water was performed in a reactor (Savannah 100, Ultratech/Cambridge Nanotech) for infiltrating the direct photonic crystals (PS templates) at 95°C. The cycle was performed under exposure mode (0.2/60/90 seconds) with nitrogen as carrier gas (30 sccm or cm^3/min). After ALD, the polymeric template was calcined in air at 500°C for 30 minutes, generating the inverse opal photonic crystal structure.

The optical response of both direct and inverse opal photonic crystals was evaluated by specular reflectance measurements (UV-vis-NIR spectrometer, PerkinElmer, Lambda 1050) from 900 to 1850 nm and at an incident angle of 8°.

3 | RESULTS AND DISCUSSION

3.1 | Visual characteristics

The direct photonic crystals fabricated by vertical convective self-assembly showed an angle-dependent reflectance behavior when interacting with visible light, as expected. As seen in Figure 1, reflected light changes from blue-green to red as consequence of the incident angle.[25]

All produced samples showed characteristic self-assembly stripes, which were expected from the vertical deposition, as described elsewhere.[3,26] The orientation of the

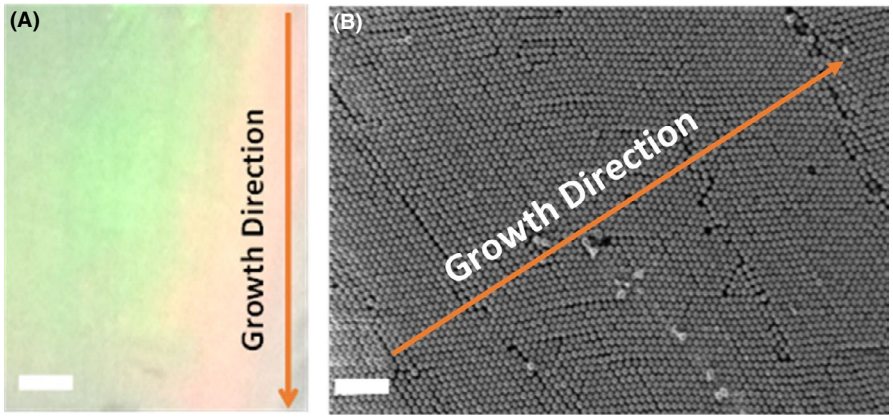

FIGURE 1 Photograph (A) and scanning electron microscopy (SEM) image (B) of a polystyrene (PS) direct photonic crystal self-assembled on a sapphire substrate at 55°C and 70% relative humidity (RH) using a PS suspension concentration of 1.5 mg/mL. Scale bars represent 8 mm and 2 μm, respectively

stripes is perpendicular to the growth direction of the crystalline layer and shows periodicity. According to Yoldi et al,[3] the stripes are formed when the meniscus draws back with a discontinuous velocity, with the surface tension embracing the meniscus. When the tension turns to be too elevated, the film ruptures and a new meniscus starts to grow, generating the stripes.

3.2 | Influence of suspension concentration

The polymer concentration plays an important role in the opal film growth. Liquid evaporation out of the thin meniscus leads to a constant influx, which draws the colloid into the area of film formation.[23] The suspension concentration controls the particles flux and, consequently, the thickness of the crystal films.[15]

As shown in Figures 2 and 3, the thickness of the produced films increases with the suspension concentration. Although a higher thickness is desired for a probable higher reflectance, a higher fraction of defects (line defects, point defects, drying cracks, stacking faults) was observed in this case.

The thickness dependence is in agreement with previous work,[15] which varied the total volume of the solvent. The increase in the thickness by tailoring the suspension concentration was also reported by McLachlan et al,[4] for polystyrene direct photonic crystals (volume variation from 1 to 5%), and also by Zhang et al[9]; the latest work presented no quantification of the density of defects.

In the current work, the increment in the direct photonic crystals' thickness generated a higher area fraction and the adhesion to the substrate was compromised, which was

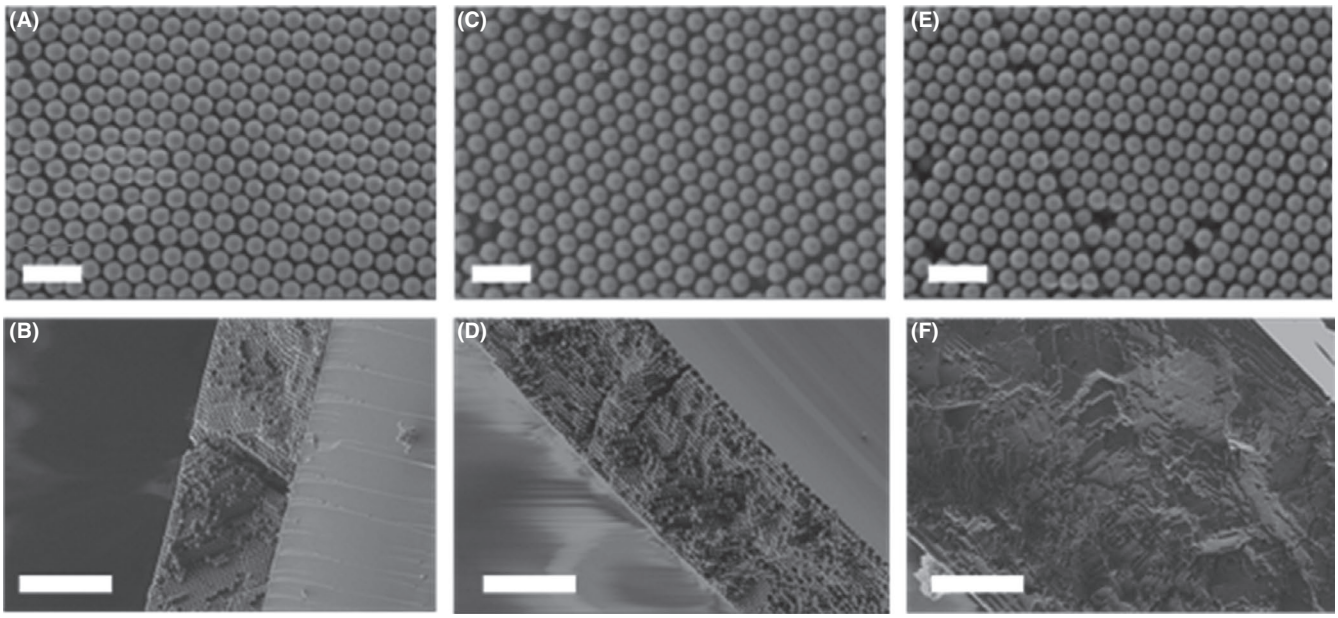

FIGURE 2 Top-view and cross-sectional scanning electron microscopy (SEM) images of polystyrene (PS) direct photonic crystals produced at 55°C and 70% relative humidity (RH) for PS concentrations of 1 (A,B), 1.5 (C,D), and 2 mg/mL (E,F). The scale bars are equivalent to 2 μm (A, C, E), 1 μm (B), 2 μm (D), and 3 μm (F)

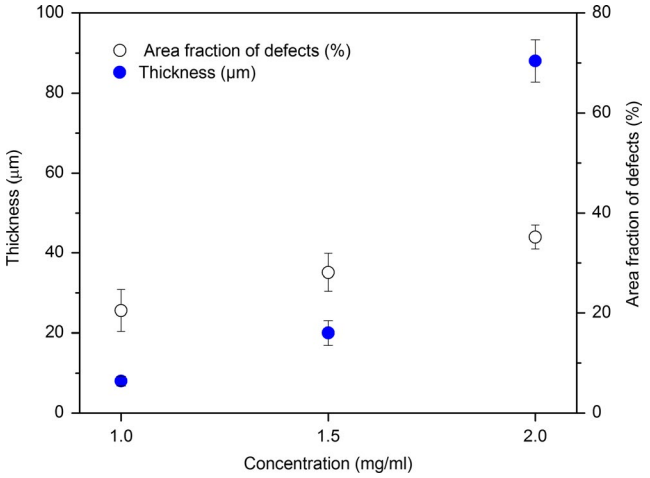

FIGURE 3 Effect of suspension concentration on the direct photonic crystals' thickness and area fraction of defects

qualitatively observed by Liu et al,[27] as well. The thickness increased from 18 to 88 μm for suspension concentrations from 1.5 to 2.0 mg/mL, which caused an increment in the density of defects. Supposedly, the defects were generated by the interactions of the particles, between the free particles still in suspension and either the substrate or the already assembled layers.

In the sequence, the reflectance was measured to support the analysis of the defects of the direct photonic crystals. Former studies such as those of Liau et al[25] and Zhou et al[20] affirm that the reflectance gets lower when the amount of defects increases, which was not observed in this work (Figure 4A). This behavior is most likely associated with the higher number of assembled layers for higher suspension concentration (see SEM image in Figure 2), as supported by some authors.[4,28–30]

3.3 | Influence of temperature

Higher temperatures raise the evaporation rate during assembly so that tensile stress within the films is increased.[31] These tensile stresses appear during drying, in which the distance between two particles increases and cracks are formed. Furthermore, the generation of vacancies also becomes more favorably generated when the evaporation rate is increased, and the particles do not have sufficient time to move to the optimal lattice site before its deposition on the substrate.[32]

The effect of the evaporation temperature was evaluated, while the suspension concentration and the relative humidity were kept at 1.5 mg/mL and 70%, respectively. The thickness and the area fraction of defects have a clear correlation with the evaporation temperature, being both increased as the temperature rises (Figure 5). It is important to point out that the self-assembly process was interrupted either after 120 hours or after total evaporation of the liquid. For the

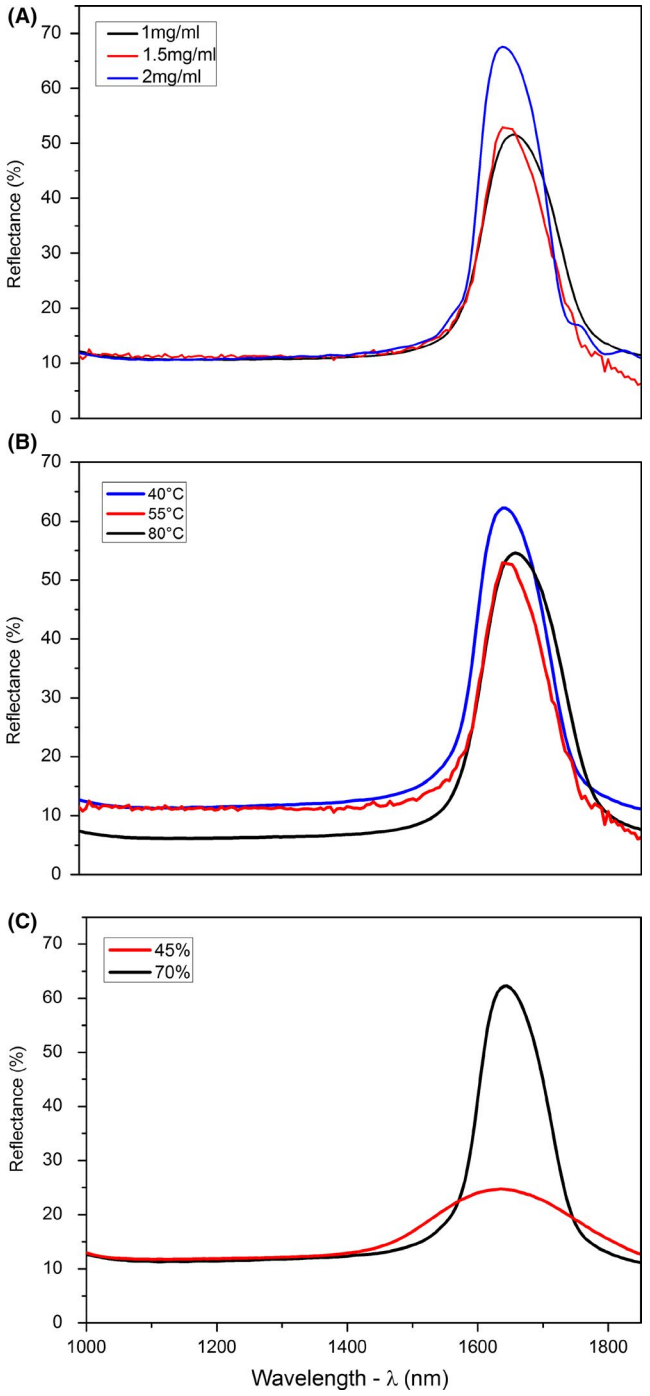

FIGURE 4 Specular reflectance measurements of the polystyrene (PS) direct photonic crystals: A, different initial concentrations (1, 1.5, and 2.0 mg/mL) at 55°C and 70% relative humidity (RH); B, different process temperatures (40, 55, and 80°C) at initial concentration of 1.5 mg/mL, and RH at 70%; C, different RH conditions (45% and 70%) at 55°C and initial concentration of 1.5 mg/mL

process performed at 80°C, the process time was 40% faster than those performed at 55 and 40°C. Although the amount of defects was higher for this condition (36% against 28% for the process at 55°C), the higher thickness obtained at reduced time could be an advantage of such high-temperature

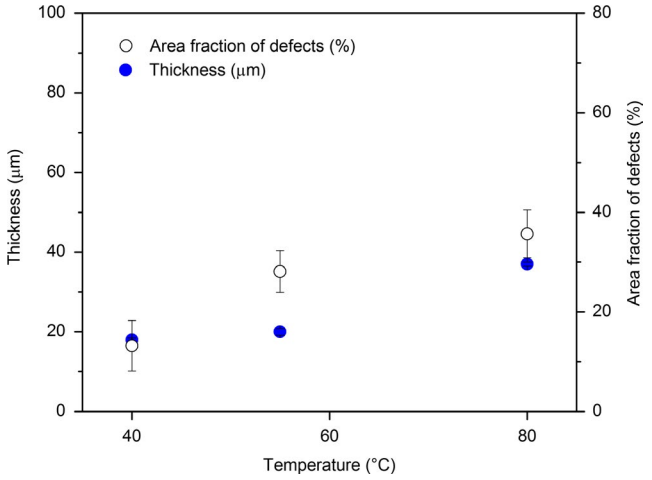

FIGURE 5 Effect of the evaporation temperature on the film thickness and area fraction of defects

self-assembly process, if the colloidal film mechanical stability and photonic response are still considered acceptable (refer to Figure 4B).

The direct photonic crystals produced at 55°C and 80°C showed more defects such as cracks and vacancies (Figure 6) than those fabricated at 40°C. The reflectance measurements support the structural evaluation of the direct photonic crystals quality (Figure 4B), as the samples produced at 40°C presented higher reflectance than those fabricated at 55 and 80°C, even though the thickness was smaller (18 μm to 20 and 37 μm, respectively). This relationship between colloidal films quality (direct photonic crystals in the present work) and evaporation temperature has been also observed qualitatively by other authors.[33,34] Chun et al,[34] compared the morphology of colloidal crystals obtained at evaporation temperatures of 45, 60 and 70°C, with constant humidity (90%). High-quality crystals with respect to ordering and reflectivity were obtained at 45°C in 24 hours, while poorly ordered structures (indicating many defects) were produced at the other two temperatures, which also corroborate these results.

In contrast, Im & Park[26] observed that the quality of the formed crystals was increased from 30 to 60°C, which was not observed in this study. However, the samples prepared at 90°C in their work also revealed significantly more defects, which is in good agreement with the trend observed here.

3.4 | Relative humidity

The influence of humidity on the ordering and defects of the direct photonic crystals can be even more critical than the pure temperature. Relative humidity influences the evaporation rate and the crystal formation.[33]

Figures 7 and 8 present the dependence of the film thickness, amount of defects, and structural ordering. The results showed that the higher the relative humidity (actively controlled by the humidity chamber), the thicker, more ordered, and less defective direct photonic crystals can be obtained. The samples fabricated with a 70% RH presented a higher reflectance than those produced with 45% (Figure 4B) strongly supporting the observation regarding suppressed defect at higher RH. Nevertheless, 90% RH was too high to allow the self-assembly, so that the corresponding data are not available. The lack of ordering in the structure is clearly visible in the cross-sectional analysis (Figure 8C), where the samples presented a more photonic glass-like appearance.[35]

In accordance with the observations of Kuai et al,[22] no self-assembly could be observed in case of 90% humidity; in this work, a decrease in the thickness of films was found for values higher than 77% RH. Furthermore, Liu et al,[5] presented similar humidity values (45, 70, and 90%) as in the present work and observed that the variation in RH resulted in the formation of many vacancies and dislocations, indicating that there probably exists an optimum point around 70%. Thereby, lower humidity promotes liquid evaporation, increasing the evaporation rate, and bringing additional internal stress, thus increasing the cracking and defects in the direct photonic crystals. At RH close to the optimum point, the lateral capillary force and slower liquid evaporation result in a better crystalline quality. Further increase in humidity reduces the evaporation rate and too weak lateral force occur

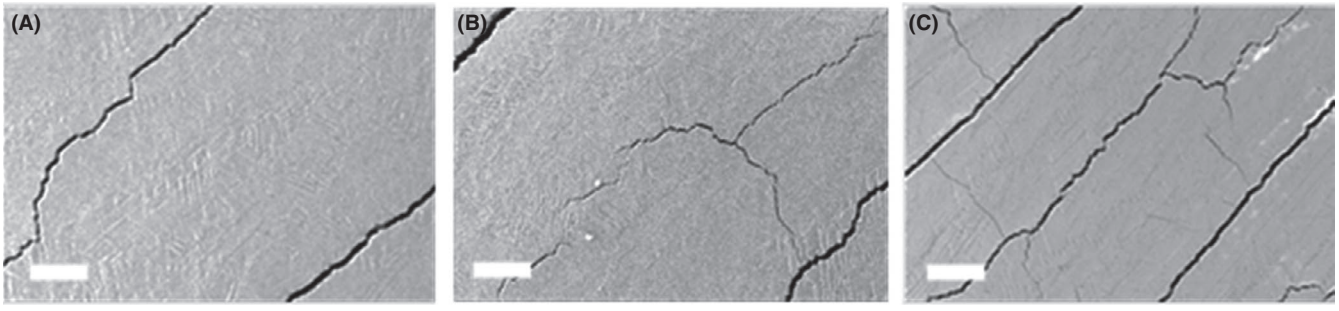

FIGURE 6 Top-view scanning electron microscopy (SEM) images of polystyrene (PS) direct photonic crystals showing the self-assembly cracks according to the process temperature (40, 55, and 80°C) using PS suspensions concentration of 1.5 mg/mL, and relative humidity (RH) kept at 70%. The scale bar represents 50 μm

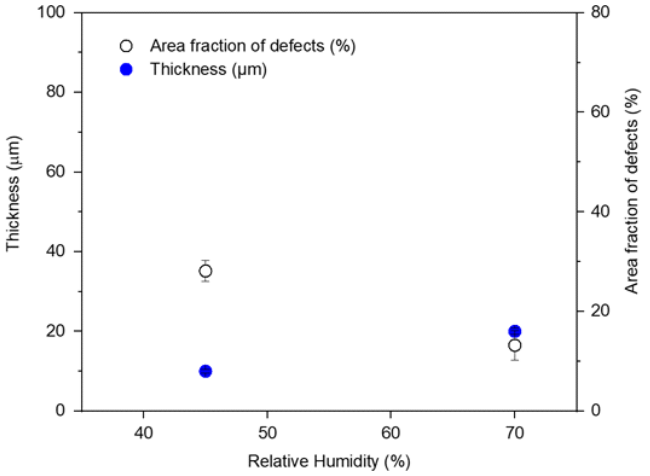

FIGURE 7 Effect of relative humidity on the film thickness and area fraction of defects

resulting in poor crystal quality. The fact that Liu et al[5] could obtain samples, even with a low quality, might be related to the chamber pressure used. In that case, a pressure of 6 kPa was applied, while the current work was performed always under atmospheric pressure.

3.5 | Oxide-based inverse opal photonic crystals

After ALD and polymer template burnout, inverse opal photonic structures of Al_2O_3 were generated[36] (insets in Figure 9). Reflectance measurements (compare them to the direct photonic crystals in Figure 4) show a blue-shift of the peak position associated with a change of the photonic band gap (Figure 10), which is related to the different structure and to

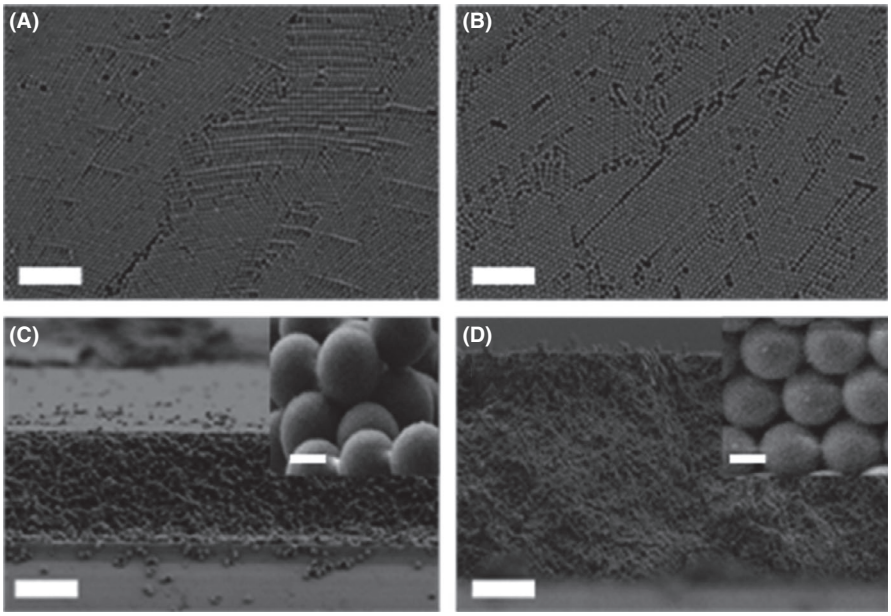

FIGURE 8 Top-view and cross-sectional scanning electron microscopy (SEM) images of polystyrene (PS) direct photonic crystals according to the relative humidity (RH) of 45% (A and C) and 70% (B and D), at 55°C and PS initial concentration of 1.5 mg/mL. In all images, the scale bars are equivalent to 2 μm. In the insets, the scale bars are equivalent to 0.25 μm

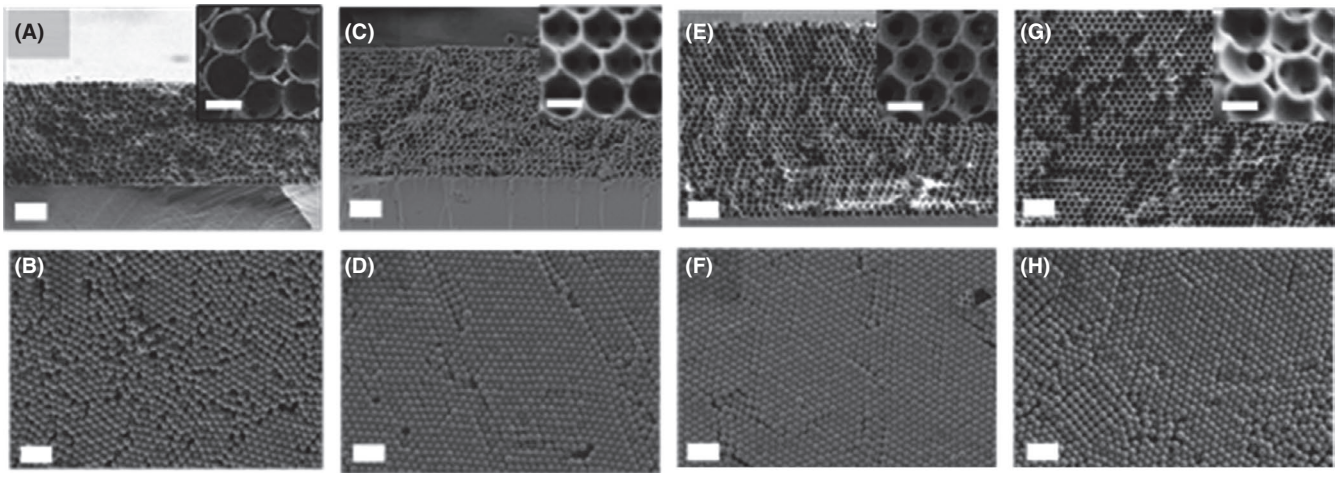

FIGURE 9 Scanning electron microscopy (SEM) images of cross section (A, C, E, and G) and top view (B, D, F, and H) of the produced alumina inverse opals. Temperature and relative humidity were, respectively, 40°C and 45% RH (A and B); 40°C and 70% (C and D); 55°C and 70% (E and F); 80°C and 70% (G and H). Scale bars represent 5 μm in the full images and 1 μm in the insets

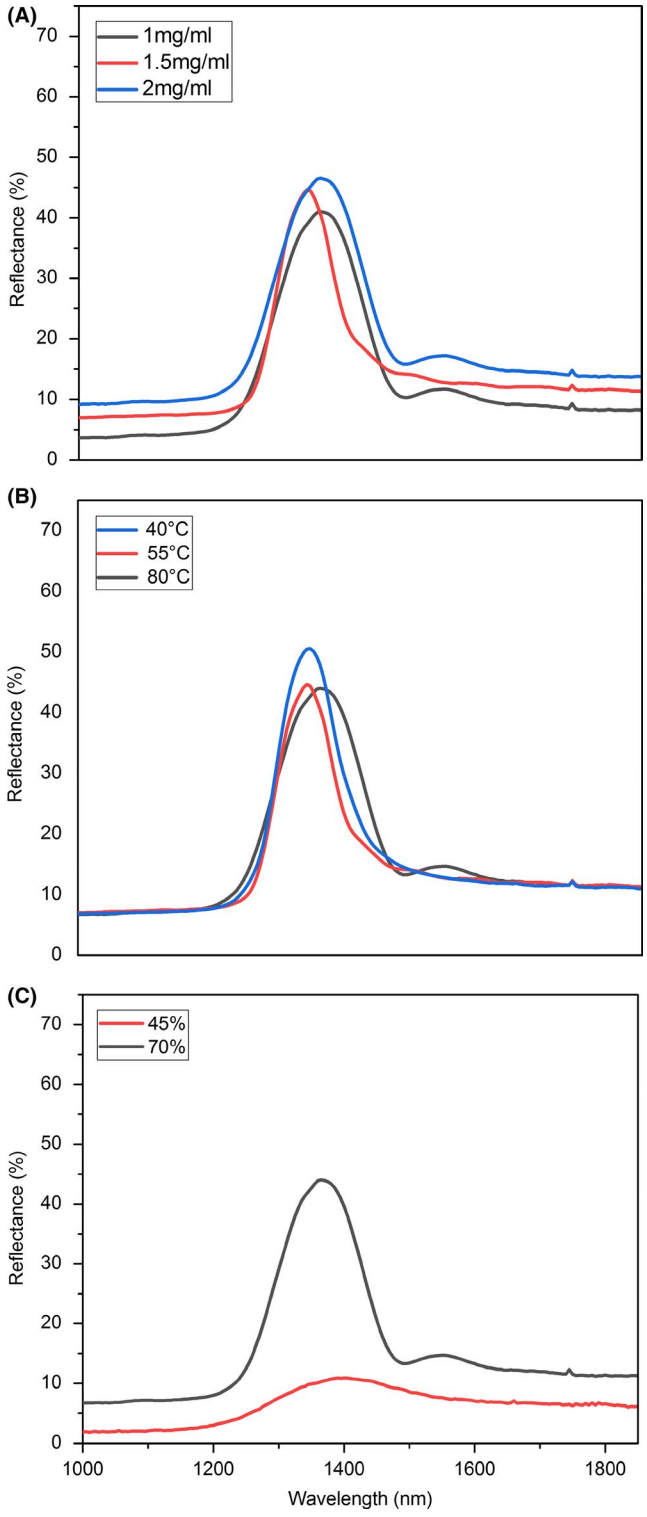

FIGURE 10 Specular reflectance measurements of the polystyrene (PS) inverse opal photonic crystals for different (A) PS suspensions initial concentration (1, 1.5, and 2.0 mg/mL) at 55°C and 70% (relative humidity [RH]); B, process temperatures (40, 55, and 80°C) at initial concentration of 1.5 mg/mL and 70% RH; C, humidity conditions (45% and 70%) at 55 °C and PS initial concentration of 1.5 mg/mL

the different refractive indexes between PS and air, or Al_2O_3 and air.[37]

Inverse opal photonic crystals present a more efficient scattering system than direct photonic crystals,[29,38] due to a larger relationship between gap-to-midgap[37] ratio. Since the inverse opal photonic crystals produced in this work presented slightly lower values for the reflectance, one can assume that an additional small number of defects, probably vacancies, faults, and cracks originated during polystyrene burnout were introduced. Zhang et al[39] investigated metallic inverse opals produced by solgel infiltration. The authors found that the defects that were already in the photonic crystal structure were magnified and some others were added after infiltration and burnout procedures. Zhang et al[39] found in the inverse opals some peculiar structural defects and called them as V, P, and H defects. V defect is a pore that is bigger than the others, P is related to deformed pores, and H is coalesced pores. Although the used materials and the infiltration method were different from the one adopted in this work, here some H defects were also found (Figure 11) in the produced inverse alumina opals. The appearance of this kind of defects and the magnification of the already existent cracks and faults may be the cause of the reflectance suppression observed when the data obtained before ALD and burnout are compared with the ones accessed after these procedures. Liau et al[25] and Zhou et al[20] also showed that an increase in the amount of the defect causes a decrease in the reflectance peak. However, these papers dealt with polymer-based direct photonic crystals only; the use of these as precursors for ceramic inverse opal photonic crystals made by ALD is not considered. Nevertheless, a correlation between those behaviors can be made and it can be concluded that the majority of defects originated during the self-assembly step remained in the structure even after ALD. Therefore, the

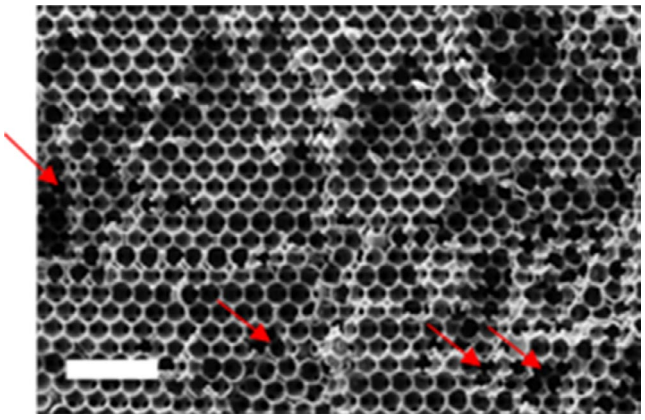

FIGURE 11 Scanning electron microscopy (SEM) image of an inverse alumina opal photonic crystal produced with 1.5 mg/mL, 55°C, 70% (polystyrene [PS] concentration, evaporation temperature, and relative humidity). The arrows show "H" defects.[37] The scale bar represents 1 μm

reflectance capability of the ceramic oxide-based inverse opal photonic crystals depends on the self-assembly parameters.

4 | CONCLUSIONS

In this work, a direct relationship between self-assembly parameters and the quality of the photonic response of the inverse opal photonic crystals (after ALD and calcination) has been disclosed. Photonic crystals of polystyrene particles were self-assembled on sapphire substrates by vertical deposition through liquid evaporation. The amount of defects in the direct photonic crystals increased with PS concentration and evaporation temperature and decreased with relative humidity up to a limit value in which self-assembly failed. The thickness was also affected by these parameters in different trends and synergistic way. The resulting reflectance capability of both direct and inverse opal photonic crystals was essentially affected by the self-assembly parameters. Although ALD and polymeric template burnout performed at 500 °C introduced some additional defects and/or enlarged preexisting defects in the structures, the self-assembly process can be considered as the main key factor influencing the resulting photonic band gap and reflectance capability. Concerning the performance of the ceramic inverse opal photonic crystals, the optimum parameters for self-assembly related to both lower defects density and substrate adhesion were 40 °C, 70% RH, and 1.5 mg/mL of suspension initial concentration.

ACKNOWLEDGMENTS

We gratefully acknowledge financial support from the German Research Foundation (DFG) via SFB 986 "M3," projects UA-UHH and C5. The authors also acknowledge financial support from the PROBRAL program, a partnership between the German Academic Exchange Service (DAAD) and the Brazilian Federal Agency for Post-graduate Education (CAPES) through the project 23038.006803/2014-50.

CONFLICT OF INTEREST

The authors declare no conflict of interest.

ORCID

Kaline P. Furlan https://orcid.org/0000-0003-4032-2795
Rolf Janssen https://orcid.org/0000-0001-7054-0510

REFERENCES

1. Xiao F-X, Miao J, Liu B. Layer-by-layer self-assembly of CdS quantum dots/graphene nanosheets hybrid films for photoelectrochemical and photocatalytic applications. J Am Chem Soc. 2014;136:1559-1569.
2. Marqués-Hueso J, Schöpe HJ. Regular Horizontal Patterning on Colloidal Crystals Produced by Vertical Deposition. In: Auernhammer GK, Butt HJ, Vollmer D, eds. Surface and Interfacial Forces - From Fundamentals to Applications. Heidelberg: Berlin, Heidelberg: Springer, Berlin; 2008:48-56.
3. Yoldi M, Arcos C, Paulke B-R, Sirera R, González-Viñas W, Görnitz E. On the parameters influencing the deposition of polystyrene colloidal crystals. Mater Sci Eng, C. 2008;28:1038-1043.
4. McLachlan MA, Johnson NP, La Rue RMD, McComb DW. Thin film photonic crystals: synthesis and characterisation. J Mater Chem. 2004;14:144. https://doi.org/10.1039/b310759k.
5. Liu GQ, Wang ZS, Ji YH. Influence of growth parameters on the fabrication of high-quality colloidal crystals via a controlled evaporation self-assembly method. Thin Solid Films. 2010;518:5083-5090.
6. Vogel N, Retsch M, Fustin C-A, Del Campo A, Jonas U. Advances in colloidal assembly: the design of structure and hierarchy in two and three dimensions. Chem Rev. 2015;115:6265-6311.
7. Xia H, Wu S, Su X, Zhang S. Monodisperse TiO2 spheres with high charge density and their self-assembly. Chem Asian J. 2017;12:95-100.
8. Wu Y, Chen C, Liu Y, Xu X, Yang Z, Zhang H, et al. Fast fabrication of a self-cleaning coating constructed with scallion-like ZnO using a perfect colloidal monolayer enabled by a predictive self-assembly method. J Mater Chem A. 2017;5:5943-5951.
9. Zhang H, Liu X. Preparation and self-assembly of photonic crystals on polyester fabrics. Iran Polym J. 2017;26:107-114.
10. Meijer J-M, Hagemans F, Rossi L, Byelov DV, Castillo SIR, Snigirev A, et al. Self-assembly of colloidal cubes via vertical deposition. Langmuir. 2012;28:7631-7638.
11. Guo P, Fan J, Cheng Y, Wang J, Wang C. Characterization of the self-assembly of glutathione stabilized cadmium selenide-zinc sulfide quantum dots with a cyanine5-labeled peptide by capillary electrophoresis and fluorescence. Anal Lett. 2017;50:197-206.
12. Fang Y, Lee WC, Canciani GE, Draper TC, Al-Bawi ZF, Bedi JS, et al. Thickness control in electrophoretic deposition of WO3 nanofiber thin films for solar water splitting. Mater Sci Eng, B. 2015;202:39-45.
13. Barros Filho DA, Hisano C, Bertholdo R, Schiavetto MG, Santilli C, Ribeiro SJL, et al. Effects of self-assembly process of latex spheres on the final topology of macroporous silica. J Colloid Interface Sci. 2005;291:448-464.
14. Liang X, Zhao Z, Zhu M, Liu F, Wang L, Yin H, et al. Self-assembly of birnessite nanoflowers by staged three-dimensional oriented attachment. Environ Sci. 2017;4:1656-1669.
15. Yan Q, Zhou Z, Zhao XS. Inward-growing self-assembly of colloidal crystal films on horizontal substrates. Langmuir. 2005;21:3158-3164.
16. Hanafusa T, Mino Y, Watanabe S, Miyahara MT. Controlling self-assembled structure of Au nanoparticles by convective self-assembly with liquid-level manipulation. Adv Powder Technol. 2014;25:811-815.
17. Bormashenko E, Whyman G, Pogreb R, Stanevsky O, Hakham-Itzhaq M, Gendelman O. Self-assembly in evaporated polymer solutions: patterning on two scales. Isr J Chem. 2007;47:319-328.
18. Mastai Y, Lidor-Shalev O, Aviv H. Assembly of ordered polystyrene nanoparticles on self- assembled monolayers. J Res Updates Polym Sci. 2016;4:202-209.

19. Teh LK, Tan NK, Wong CC, Li S. Growth imperfections in three-dimensional colloidal self-assembly. Appl Phys A. 2005;81:1399-1404.
20. Zhou L, Wu Y, Chai L, Liu G, Fan Q, Shao J. Study on the formation of three-dimensionally ordered SiO 2 photonic crystals on polyester fabrics by vertical deposition self-assembly. Text Res J. 2016;86:1973-1987.
21. Zhang J, Sun Z, Yang B. Self-assembly of photonic crystals from polymer colloids. Curr Opin Colloid Interface Sci. 2009;14:103-114.
22. Kuai S-L, Hu X-F, Haché A, Truong V-V. High-quality colloidal photonic crystals obtained by optimizing growth parameters in a vertical deposition technique. J Cryst Growth. 2004;267:317-324.
23. Weiss D, Kreger K, Schmidt H-W. Self-assembly of alkoxy-substituted 1,3,5-benzenetrisamides under controlled conditions. Macromol Mater Eng. 2017;302:1600390.
24. Voïtchovsky K, Giofrè D, José Segura J, Stellacci F, Ceriotti M. Thermally-nucleated self-assembly of water and alcohol into stable structures at hydrophobic interfaces. Nat Commun. 2016;7:13064.
25. Liau LC-K, Huang Y-K. Effects of influential factors on sedimentation self-assembly processing of photonic band gap crystals by relative humidity-controlled environments. Chem Eng Process. 2008;47:1578-1584.
26. Im SH, Park OO. Effect of Evaporation Temperature on the Quality of Colloidal Crystals at the Water−Air Interface. Langmuir. 2002;18:9642-9646.
27. Liu T-T, Tian W, Song Y-L, Bai Y, Wei P-L, Yao H, et al. Reversible self-assembly of backbone-thermoresponsive long chain hyperbranched poly(N-isopropyl acrylamide). Polymers. 2016;8:33.
28. Hilhorst Jan, van Schooneveld Matti M, Wang Jian, de Smit Emiel, Tyliszczak Tolek, Raabe Jörg, et al. Three-dimensional structure and defects in colloidal photonic crystals revealed by tomographic scanning transmission X-ray microscopy. Langmuir. 2012;28:3614-3620.
29. Lee HS, Kubrin R, Zierold R, Petrov AY, Nielsch K, Schneider GA, et al. Thermal radiation transmission and reflection properties of ceramic 3D photonic crystals. J Opt Soc Am B. 2012;29:450.
30. Nandiyanto ABD, Suhendi A, Arutanti O, Ogi T, Okuyama K. Influences of surface charge, size, and concentration of colloidal nanoparticles on fabrication of self-organized porous silica in film and particle forms. Langmuir. 2013;29:6262-6270.
31. Bogue R. Self-assembly: a review of recent developments. Assembly Autom. 2008;28:211-215.
32. Xavier J, Dasgupta R, Ahlawat S, Joseph J, Gupta PK. Controlled formation and manipulation of colloidal lattices by dynamically reconfigurable three dimensional interferometric optical traps. Appl Phys Lett. 2012;101:201101.
33. Chhasatia VH, Joshi AS, Sun Y. Effect of relative humidity on contact angle and particle deposition morphology of an evaporating colloidal drop. Appl Phys Lett. 2010;97:231909.
34. Chung Y-W, Leu I-C, Lee J-H, Hon M-H. Influence of humidity on the fabrication of high-quality colloidal crystals via a capillary-enhanced process. Langmuir. 2006;22:6454-6460.
35. García PD, Sapienza R, López C. Photonic glasses: a step beyond white paint. Chem Rev. 2010;22:12-19.
36. Wang J, Yang L, Lin D, Luo Y, Li D, Meng Q. Optical studies of random disorder of colloidal photonic crystals and its evolution in evaporation induced self-assembly. J Chem Phys. 2012;137:234111.
37. John S, Busch K. Photonic bandgap formation and tunability in certain self-organizing systems. J Lightwave Technol. 1999;17:1931-1943.
38. Furlan KP, Pasquarelli RM, Krekeler T, Ritter M, Zierold R, Nielsch K, et al. Highly porous α-Al 2 O 3 ceramics obtained by sintering atomic layer deposited inverse opals. Ceram Int. 2017;43:11260-11264.
39. Zhang X, Blanchard GJ. Polymer sol-gel composite inverse opal structures. ACS Appl Mater Interfaces. 2015;7:6054-6061.

How to cite this article: Campos HG, Furlan KP, Garcia DE, et al. Effects of processing parameters on 3D structural ordering and optical properties of inverse opal photonic crystals produced by atomic layer deposition. *Int J Ceramic Eng Sci*. 2019;1: 68–76. https://doi.org/10.1002/ces2.10015